U. of Iowa 65-12

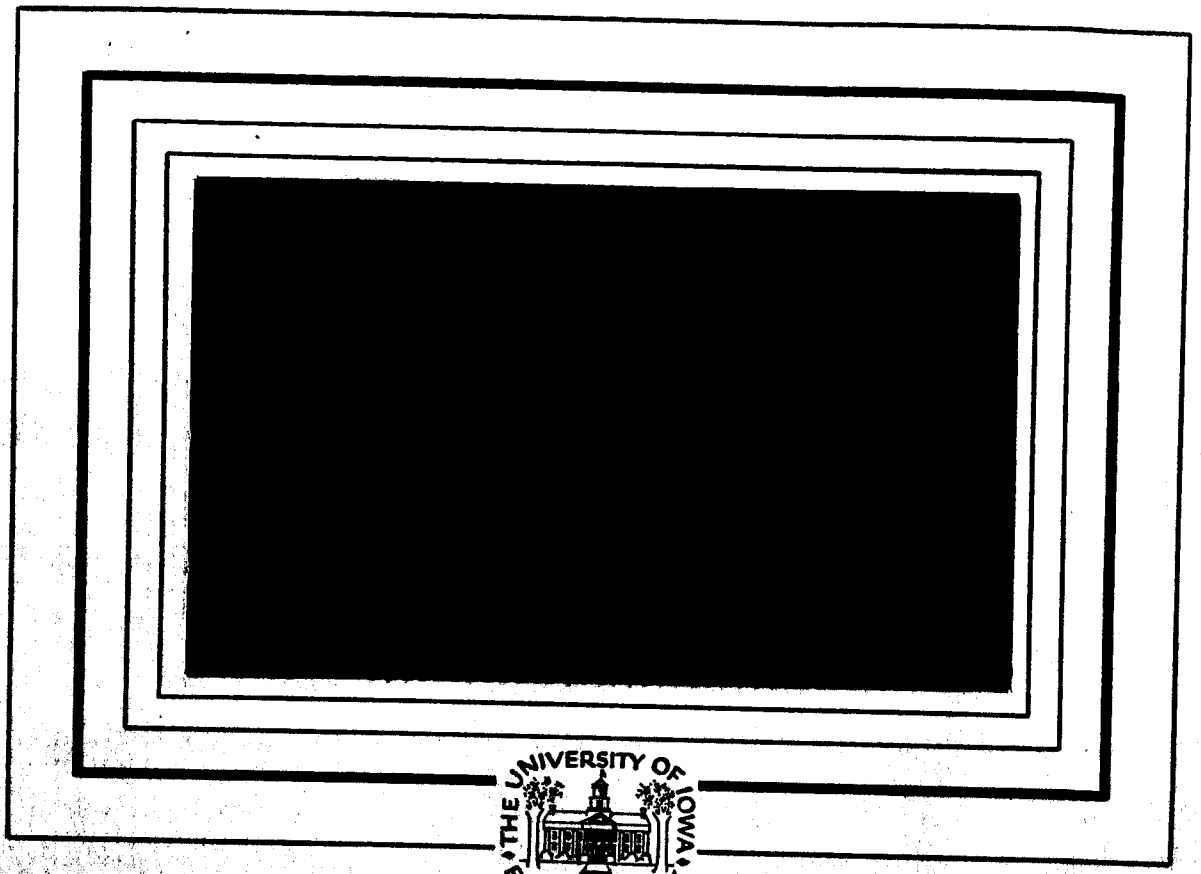

Department of Physics and Astronomy
THE UNIVERSITY OF IOWA
Iowa City, Iowa

U. of Iowa 65-12

Light Density and Color Distribution in the Earth's Shadow*

by

James E. Hansen** and Satoshi Matsushima
University of Iowa Observatory
Iowa City, Iowa

April 1965

*Work supported in part by a grant from the National Science Foundation.

**Graduate Trainee of the National Aeronautics and Space Administration.

ABSTRACT

After taking into account the solar limb-darkening, the light density and color in the earth's shadow are computed by performing a double numerical integration over the atmosphere. As sources of light attenuation, ozone absorption and extinction by dust and clouds are taken into account in addition to the usual Rayleigh scattering and the refraction weakening. Molecular diffusion and diffusion by dust and water particles are also included in the calculations. Special emphasis is placed on finding an explanation for the unusual eclipse of December 30, 1963, in which an extremely low light density and an apparent non-reddening were observed.

Calculations are carried out for various models of the earth's atmosphere and it is shown that the dust particles may account for large changes in the light density from eclipse to eclipse. The dust and clouds appear to cause the non-reddening by enhancing the importance of the diffused light in the central region of the earth's shadow. The observation of the 1963 eclipse is found to be explained by assuming an abnormally large extinction presumably caused by dust spread by the eruption of Mt. Agung on March 17, 1963. The required additional extinction amounts to 0.14 magnitudes per air mass in the visible region,

which agrees with direct measurements of visual extinction made at Cerro Tololo and Mt. Bingar during the year 1963. It is also shown that the theory provides a conclusive means of distinguishing between extinction due to dust particles and that due to clouds. An approximate value for the amount of ozone in the atmosphere may also be determined. The results suggest useful plans for photometric observations of future eclipses of the moon.

I. INTRODUCTION

An unusually dark eclipse of the moon was observed on December 30, 1963. The three color photometric observations of Matsushima and Zink [1964] showed that at mid-totality the moon was darkened by about 16.25 magnitudes in all three colors, indicating an absence of the usually conspicuous reddening in the umbral region. The cause of this observed darkening, which was about 4 magnitudes greater than that of a normal eclipse, has been generally attributed to the increase in extinction due to dust particles spread through the upper atmosphere by the volcanic explosions of Mt. Agung on the island of Bali in March, 1963. The purpose of this paper is to investigate the effect of dust extinction by calculating the density and color distributions of the umbral light for various detailed models of the earth's atmosphere. These computations were made first with the IBM 7040 and later with the 7044 at the Computer Center of the University of Iowa. The entire set of calculations is carried out for blue (λ 0.46 μ), green (λ .54 μ), and red (λ .62 μ) regions.

The principal sources of attenuation of light passing through the atmosphere are refraction weakening, which simply spreads the light over a wider area, and extinction which

actually removes a fraction of the light from the incident beam. In extinction are included both the scattering and absorption of light by various particles in the atmosphere. Link [1963] has derived equations giving the intensity of light in the umbra for light emitted from a point source, accounting for refraction and Rayleigh scattering, as a function of the minimum altitudes of the rays in the earth's atmosphere. The fundamental principle of the calculations is based on Link's method with necessary modifications being made to take into account ozone absorption and scattering by dust and water particles. The brightness distribution over the sun's disk is expressed in terms of the limb-darkening coefficients, and the desired light density then obtained by performing a double numerical integration over the sun's surface. Further, the work of Svestka [1948] is used to include the density of light contributed by molecular diffusion, and calculations are also made to add the diffusion due to dust particles.

II. INTEGRATION OF THE LIGHT DENSITY

In order to find the light density at a single point in the earth's shadow, it is necessary to integrate over the surface of the sun. As will be shown, this process is equivalent to an integration over the atmosphere of the earth. In Figure 1, P_m is an arbitrary point on the plane perpendicular to the shadow axis SEM and containing the center of the moon. Assuming the earth's atmosphere to be spherically symmetric, a light ray passing from the point P_m through the earth's atmosphere with a minimum altitude h_o must strike the plane of the sun somewhere on the circle containing the point P_s. Now the converse is also true; light emitted from a point on this circle and passing through the earth's atmosphere with minimum altitude h_o must strike the point P_m on the plane of the moon. ω is the total angle of refraction for the light ray with minimum altitude h_o.

Let e_λ be the quantity which is being sought, namely the brightness or illumination at the arbitrary point P_m. Then an element dS of the sun's surface at P_s produces an illumination at P_m given by

$$d\, e_\lambda = k\, b_\lambda\, T_\lambda\, dS \qquad (1)$$

where b_λ is the surface brightness of the sun at the point P_s, T_λ is the tramsmission coefficient of the ray which begins at

P_s and ends at P_m including all types of weakening such as that due to refraction, ozone, dust, and Rayleigh scattering, and k is a function of the relative positions of the three bodies being considered. In the short period of an eclipse k is nearly constant, and, as will be shown, it cancels from the quantities of interest. The light density at P_m is calculated by the following integration over the surface of the sun, as illustrated in Figure 2.

$$e_\lambda (G) = 2k \int_{r=G-R_s}^{G+R_s} \int_{\epsilon=0}^{\epsilon_o} b_\lambda(R)\, T_\lambda(r)\, r\, dr\, d\epsilon, \quad (2)$$

where G is the angular distance of the point E_s from the center of the sun and is also equal to the angular distance of P_m from the center of the umbra M (Figure 1). R_s is the angular radius of the sun and $b_\lambda(R)$ represents the solar limb darkening. The factor 2 is due to the integration parameter ϵ as defined in Figure 2.

In the absence of the earth, that is, outside of eclipse, $T_\lambda(r) = 1$ and the brightness would be

$$E_\lambda = 2k \int_{G-R_s}^{G+R_s} \int_{0}^{\epsilon_o} b_\lambda(R)\, r\, dr\, d\epsilon. \quad (3)$$

The logarithm of the ratio E_λ/e_λ gives the density of the shadow on the stellar magnitude scale

$$D_\lambda = \log_{2.512} E_\lambda/e_\lambda \, . \tag{4}$$

The surface brightness on the sun, $b_\lambda(R)$, may be expressed in terms of the integration variables through

$$b_\lambda(R) = A_\lambda + B_\lambda (G^2 + r^2 - 2r\, G \cos \epsilon)^{1/2} + C_\lambda (G^2 + r^2 - 2r\, G \cos \epsilon), \tag{5}$$

where A_λ, B_λ, and C_λ denote the limb darkening coefficients defined by

$$\frac{I_\lambda(\theta)}{I_\lambda(0)} = A_\lambda + B_\lambda \sin\theta + C_\lambda \sin^2\theta \, .$$

The principal advantage in the above method of integration lies in the form of the transmission factor T_λ for the ray traveling from P_s to P_m. Under the assumption of a spherically symmetric atmosphere T_λ is a function of the minimum altitude h_o and there is a one to one correspondence between h_o and the angle r. Hence

$$T_\lambda = T_\lambda(r) = T_\lambda(h_o) \, . \tag{6}$$

For this reason it is equally precise to say that the integration is over the surface of the sun or that it is over the earth's atmosphere. It is convenient to write

$$T_\lambda(r) = T_\lambda^R(r)\, T_\lambda^r(r)\, T_\lambda^O(r)\, T_\lambda^A(r)\, T_\lambda^W(r) \qquad (7)$$

where the superscripted T's represent the contributions to the transmission factor from each of the five dominant types of extinction--Rayleigh, refraction, ozone, aerosol, and water particle (cloud), respectively.

III. REFRACTION AND AIR MASS FOR LIGHT PASSING PARALLEL TO THE EARTH'S SURFACE

In order to compute both the change in intensity of light due to refraction and the decrease in intensity due to extinction of all possible types, the path of the light rays through the earth's atmosphere must be known. The usual astronomical formulae for refraction may not be used since they are not valid for large zenith distances and in the lunar eclipse the rays of interest are those with a zenith distance of 90 degrees, that is, rays passing parallel to the earth's surface. This refraction problem was first considered extensively by Link [1963] and his theory is used here with some modifications.

In addition to the minimum height h_o, we introduce another parameter h_o' designating the minimum altitude of the same ray if it were not refracted (Figure 1). Further letting ρ be the relative density of the air such that $\rho = 1$ for 0° C and 760 mm Hg the relative density gradient α is defined by

$$\alpha = \frac{1}{\rho} \left| \frac{d\rho}{dh} \right| . \tag{8}$$

For the present problem the index of refraction of air may be expressed by the approximate formula

$$\mu_\lambda = 1 + C_\lambda \rho \tag{9}$$

where $C_\lambda \tilde{=} .00029$ for the wavelengths under consideration.

Link [1963] has shown that if z is the angle between the light ray's path at the altitude h and a radial element from the earth's center intersecting the path at the point h then the total refraction of the ray in the earth's atmosphere is given by

$$\omega = 2 \int_{h=h_o}^{h=\infty} \frac{\tan z}{\mu (h)} \, d\mu . \tag{10}$$

Using Snell's law and the Invariant Theorem [Humphreys, 1940], it follows that z is given by

$$\sin z = \frac{\mu_o (R_o + h_o)}{\mu (R_o + h)} \tag{11}$$

where R_o is the radius of the earth and μ_o is the index of refraction at $h = h_o$. If h and h_o are measured in terms of the earth's radius ($R_o = 1$) then

$$\sin z = \frac{(1 + C \rho_o)(1 + h_o)}{(1 + C \rho)(1 + h)}$$

$$\simeq 1 - (h - h_o) + C (\rho_o - \rho) . \tag{12}$$

Using this approximation and introducing a parameter y defined by

$$y = \cos z,$$

the total refraction may be expressed as

$$\omega = 2 \int_0^1 \frac{C \rho \alpha}{1 - C\rho\alpha} \, dy . \tag{13}$$

ω is one of the three basic integrals which must be computed numerically as a function of the light ray's minimum altitude in the atmosphere. The second is the gradient of ω which is given by [Link, 1963]

$$\frac{d\omega}{dh'_o} = -2 \int_0^1 \frac{1}{1 - C\rho\alpha} \frac{dK}{dh} \, dy \tag{14}$$

where

$$K = \frac{C\rho\alpha}{1 - C\rho\alpha} .$$

Both ω and the gradient of ω appear in the calculation of the refraction weakening (see equation (19)).

The third integral is the total air mass along the ray path as a function of its minimum altitude h_o. This is given by

$$M = 2 \int_{h_o}^{\infty} \rho \sec z \, dh = 2 \int_0^1 \frac{\rho \operatorname{cosec} z}{1 - C\rho\alpha} \, dy$$

$$\simeq 2 \int_0^1 \frac{\rho}{1 - C\rho\alpha} \, dy . \tag{15}$$

The numerical computations of these integrals (13), (14), and (15) were carried out by taking the atmospheric density for each one-half kilometer tabulated in the United States Standard Atmosphere [Champion et al., 1962]. The results for the total refraction ω, the gradient of ω, and the horizontal air mass M, each as a function of altitude, are tabulated in the first four columns of Table I.

With the above quantities known, the relation between r and h_o becomes a matter of geometry. The following relation is readily obtained [Link, 1963],

$$r = (\pi_m + \pi_s)\left(1 + \frac{h'_o}{R_o}\right) - \omega , \qquad (16)$$

where π_m and π_s are the geocentric parallax of the moon and of the sun, respectively.

IV. SOURCES OF ATTENUATION OF LIGHT

A. Rayleigh Scattering

The Rayleigh extinction may be accounted for by the factor

$$T_\lambda^R = e^{-A_\lambda M} \tag{17}$$

where A_λ is the Rayleigh extinction coefficient for a unit air mass. The calculation of M, the air mass along the tangential path, was described in the preceding section while A_λ is the product of the reduced equivalent thickness of the atmosphere (7.995 km) and the Rayleigh scattering coefficient given by [Campen, 1961]:

$$\sigma_\lambda = \frac{32\pi^3 (\mu - 1)^2}{3 n \lambda^4} \tag{18}$$

where n is the number of scattering particles per unit volume at STP. σ_λ is tabulated by Penndorf [1957].

B. Refraction Weakening

The expression for refraction weakening, T_λ^r, is readily obtained from the geometry and from equation (16) to be the following [Link, 1963]:

$$T_\lambda = \left[1 - \frac{\omega}{\pi_m + \pi_s} \left(1 - \frac{h'_o}{R_o}\right) \right] \left[1 - R_o \frac{d\omega}{d h'_o} \frac{1}{\pi_m + \pi_s} \right] . \tag{19}$$

Thus T_λ^r for a given minimum altitude h_o may be computed from the above equation, using the values of ω and $d\omega/d\, h_o'$ tabulated in the second and third columns of Table I.

C. Ozone Absorption

The calculation of the ozone absorption T_λ^o is not difficult if the vertical distribution of ozone, $o(h)$, is known. The function $o(h)$ is defined to be the equivalent path length of pure ozone at 0° C and 760 mm which is contained in 1 km of air at the altitude h. Then the "total amount" of ozone passed through by a ray with minimum altitude h_o, which is designated by $O(h_o)$, is given by an expression similar to that used in computing the air mass (equation (15)):

$$O(h_o) = 2 \int_{h_o}^{\infty} o(h) \sec z \, d\, h \, . \qquad (20)$$

In this case, however, we note that the refraction of the light ray in the high atmospheric region of the ozone layer is very small, and we can simplify the integration corresponding to equation (15) by taking a straight line for the ray's path. Then since

$$\sec z \simeq \sqrt{\frac{R_o}{2\,(h - h_o)}} \qquad (21)$$

we can write

$$O(h_o) = \sqrt{2 R_o} \int_{h_o}^{\infty} \frac{o(h)}{\sqrt{h - h_o}} \, dh . \quad (22)$$

For the vertical density of ozone, o(h), the following empirical formula derived by Green [1964] is used:

$$o(h) = \frac{P_1}{P_2} \frac{e^{P(h)}}{\left\{1 + e^{P(h)}\right\}^2} \quad (23)$$

where

$$P(h) = \frac{h - P_3}{P_2} .$$

The three adjustable parameters, P_1, P_2, and P_3, may be selected so that the shape of the distribution curve agrees with the observed form of the ozone layer. From the standard density distribution of ozone for middle latitude proposed by Altshuler [1961], the values of .22, 4.6, and 23.0 are obtained for P_1, P_2, and P_3, respectively.

Using equations (22) and (23) the quantity $O(h_o)$ has been computed numerically for each kilometer from 0 to 100. The calculations have been carried out with the following two values of vertical ozone content,

$$\int_0^\infty o(h)\,dh = .26 \text{ cm S.T.P. and } .36 \text{ cm S.T.P.},$$

for reasons to be discussed later (Section IX). The results for $O(h_o)$ are tabulated in the last two columns of Table I.

T_λ^O follows from the tabulated values for $O(h_o)$ since it may be expressed as

$$T_\lambda^O = e^{-k_\lambda O(h_o)} \tag{24}$$

where k_λ is the ozone absorption coefficient. The experimental values of k_λ at normal pressure and at a temperature of 18° C have been found by Inn and Tanaka [1953]. The values used are:

λ = 4600 A	k_λ = .0069
λ = 5400 A	k_λ = .071
λ = 6200 A	k_λ = .104

Although k_λ is a function of temperature, no corrections are necessary since as Vigroux [1953] has shown the variation is only one percent between -92° C and 50° C for the wavelengths considered here.

D. Aerosol Extinction

The extinction cross section of a single spherical particle of radius a may be written as

$$C_{ext}(a) = \pi a^2 Q_{ext}(a) \qquad (25)$$

in which the efficiency factor Q_{ext} is defined. If there are $n(a,h)da$ particles per cm^3 with radii in the interval between a and a+da at the height h, then the total number of particles included in the tangential path of light rays with 1 cm^2 cross section and minimum height, h_o, may be written as

$$N(h_o) = 2 \int_{h_o}^{\infty} \int_{o}^{\infty} n(a,h) \sec z \, da \, dh , \qquad (26)$$

or by substituting (21), we have

$$N(h_o) \cong \sqrt{2 R_o} \int_{h_o}^{\infty} \int_{o}^{\infty} n(a,h) (h - h_o)^{-1/2} \, da \, dh . \qquad (27)$$

Hence the aerosol extinction factor, T_λ^A, may be obtained by combining equations (25) and (27) as follows:

$$T_\lambda^A = \exp \left\{ - \pi \sqrt{2 R_o} \int_{h_o}^{\infty} \int_{o}^{\infty} n(a,h) (h - h_o)^{-1/2} a^2 Q_{ext}(a) \, da \, dh \right\} . \qquad (28)$$

The computations of the efficiency factor Q_{ext} for spherical particles are carried out by van de Hulst [1957] in terms of a

parameter $x = 2\pi a/\lambda$ and the refractive index of the particles. If the refractive index is assumed to be the same for all the particles then Q_{ext} is a function of x only and the color dependency in the aerosol extinction enters through this parameter. It is found that for $x < 1$, which for the wavelengths under consideration corresponds approximately to a < 0.1 micron, the efficiency factor decreases very rapidly as x decreases below unity. For example, for a non-absorbing sphere some representative values from van de Hulst are:

$x = 1.0$	$Q = 2.036$
$x = .5$	$Q = .218$
$x = .1$	$Q = .00034$

From the above figures, from the fact that the extinction coefficient involves the square of the particle radius, and from the normal aerosol size distribution [Campen, 1961], it is apparent that even though Aitkin particles ($a < .1$ micron) are the most numerous their contribution to the total extinction is negligible. For particles with $a > 1.0$ micron, Q_{ext} is very nearly constant and equal to 2.0 and therefore the extinction is neutral. Hence only for particles with $.1\ \mu < a < 1.0\ \mu$ is there a possible direct color effect. However, since the Q-values fluctuate in this range and since there is in general a continuous

range of particle sizes, the color effects largely cancel and for the accuracies obtainable in eclipse observations the assumption of neutral extinction may be justified. In fact, from the extensive measurements of extinction coefficients and photoelectric spectral scanning observations for about 18 months after the eruption of Mt. Agung, Moreno, Senduleak, and Stock [1965] concluded that the volcanic dust is a neutral scattering agent. Further from the analysis of various direct measurements made after the eruption, it has been found that n (a,h) decreases rather sharply from a maximum which occurs with the radius between 0.5 and 0.8 microns [Matsushima, 1965].

Under the assumption of neutral extinction an average particle radius a_o may be introduced and equations (27) and (28) will be simplified to:

$$N(h_o) = \sqrt{2 R_o} \int_{h_o}^{\infty} n(h) (h - h_o)^{-1/2} dh \qquad (29)$$

and

$$T_\lambda^A = \exp \left\{ - \sqrt{2 R_o} \cdot \pi a_o^2 Q_{ext}(a_o) N(h_o) \right\} . \qquad (30)$$

In practice, the variations of the aerosol extinction with the different models for the particles' vertical distribution can

be investigated in a manner similar to the method applied for other extinction factors described in the preceding sections, namely, the aerosol extinction in the tangential direction can be expressed in terms of the extinction coefficient in the zenith direction:

$$\beta = \pi a_o^2 N_o Q_{ext} , \tag{31}$$

where

$$N_o = \int_o^\infty n(h)\, dh . \tag{32}$$

Then T_λ^A may be written in analogy to the ozone factor T_λ^o as

$$T_\lambda^A (h_o) = e^{-\beta L(h_o)} \tag{33}$$

where

$$L(h_o) = N(h_o)/N_o \tag{34}$$

is the ratio of the total number of particles contained in a tangential cylinder of unit cross section with minimum height h_o to the total number of particles in a vertical column of the same cross section. This method of expression is especially advantageous when a number of different models with the same $L(h_o)$ are considered. For example, if we assume models each

having an homogeneous distribution of dust particles and the same upper limit but a different density or average particle size, then from equation (29) $L(h_o)$ is given by the simple geometric factor

$$L(h_o) = 2\sqrt{2 R_o (H - h_o)} / H \qquad (35)$$

where H is the height of the upper limits of the dust layers. Thus, since $L(h_o)$ is independent of the number density, n_o, and the mean radius of particles, a_o, each of the different models under consideration may be expressed by changing a single parameter β. If the vertical extinction coefficient β is determined from standard photometric observations, therefore, we have a means to check the adopted model of the dust layer independently.

E. Cloud Extinction

In addition to the usual dust and haze, a varying content of water particles (clouds) generally contributes to the atmospheric extinction, although the absorption by molecular water vapor in a clear sky is less than 1% of the total extinction in the visible region [Allen, 1963]. Since the central region of the earth's shadow is illuminated at any point by a wide area of the terminator

region around the earth, bad weather conditions at various local areas may generally cause a considerable degree of extinction.

The variation of extinction due to the weather conditions in the lower atmosphere may be accounted for by considering spherical water particles of average size a_o. Then the basic equations become the same as in the case of aerosol extinction discussed above. T_λ^W in (7) will be given by an equation corresponding to (30), in which $N(h_o)$ designates the total density of such particles along the horizontal direction with minimum height, h_o.

V. DIFFUSION OF LIGHT

Diffusion of light by the molecules and dust particles in the atmosphere is an additional physical process which in some cases adds a significant contribution to the light density in the earth's shadow. It is especially important in dark eclipses such as the one of December 1963. The molecular diffusion has been calculated by Svestka [1948] with the results for a lunar parallax of 61' being given below.

$\lambda = 4500$ A $\qquad M_{diff} = 16.53$

$\lambda = 7000$ A $\qquad M_{diff} = 16.68$

Because the difference in M_{diff} for these extreme wavelengths is small, and because from Svestka's equations it is obvious that the change is continuous, it is permissible to interpolate for the intermediate wavelengths.

Since the 1963 eclipse was unusually dark presumably because of dust in the atmosphere it is important to also consider the possible diffusion of light by such particles. With only a slight modification, an equation of Svestka may be used to find the density due to dust diffusion, D_{diff}, in particular

$$D_{diff} = \frac{3 W_m^2}{4 R_o} \int_{H_1}^{H_2} e^{-\beta D(h_o)} \beta D(h_o) dh_o \qquad (36)$$

where H_1 and H_2 are respectively the lower and upper limits of the dust layer. The exact result depends upon the model used for the dust layer but a typical result is $D_{diff} \simeq 17.2$ magnitudes and for all models investigated the dust diffusion is found to be less than 17 magnitudes.

VI. NUMERICAL RESULTS

A. Rayleigh and Ozone Atmosphere

In order to investigate the relative contribution of Rayleigh scattering as compared to the other sources of extinction, we first computed the shadow density for a simple Rayleigh atmosphere by setting $T^O = T^A = T^W = 1.0$ in equation (7). The result is shown in Figure 3. The contribution of molecular diffusion is appreciable only in blue wavelengths near the central region of the umbra and is shown by the broken line in Figure 3. The shadow in this case is red throughout but in reality there is always some ozone present which must be accounted for.

The vertical ozone content is variable in both season and latitude, ranging between about 0.21 cm S.T.P. and 0.38 cm S.T.P. [Albright, 1939]. The average content in winter or summer near middle latitude regions is estimated to be 0.26 cm S.T.P. For the December 1963 eclipse observations of Matsushima and Zink [1964] the effective part of the earth's terminator was located in the South Pacific Ocean when both the season and latitude would supposedly cause a relatively high content. Therefore calculations were made for both the normal content of .26 and a high content of .36 cm S.T.P. The results, including

molecular diffusion, are plotted in Figure 4. The effect of increasing the ozone content appears to be appreciable in red and green but insignificant in the blue region. It appears, therefore, that accurate measurements in the red color near the outer region of the umbra could provide a means of determining the amount of ozone in the atmosphere. The central region may not be used for this purpose since the diffusion effect tends to neutralize the color in that area as will be discussed later.

The two models in Figure 4 give the value of blue minus green (B-V) at the point 10 minutes from the umbra center to be 3.65 and 3.85 for the high and low ozone content, respectively. Since Matsushima and Zink determined the B-V color near mid-totality to be slightly negative it is apparent that the aerosol extinction must be taken into account for that eclipse.

B. Aerosol and Cloud Extinction

The vertical distribution of aerosols in the micron size range shows considerable variations especially in the lower altitude, depending on the place and time of observations. A series of recent observations by means of high altitude balloon flights has shown the stratospheric aerosols extend up to 30 km with a maximum at an altitude between 15 and

17 km [Rosen, 1964 and 1965]. Below this maximum the aerosol density decreases sharply in the tropospheric region reaching a minimum between 5 and 10 km. The observed sink between 5 to 10 km appears to be caused by rain washing effects in the tropopause and the density variations become especially noticeable in the region below 5 km. The preliminary result of a detailed analysis of the data taken during the years 1963 and 1964 near Minneapolis seems to indicate an additional source of aerosols, presumably the volcanic dust ejected into the stratosphere by the eruption of Mt. Agung [Matsushima, 1965]. From observations of the unusual reddening of the sky at sunset, Meinel and Meinel [1964] and others also estimated that the dust of assumed volcanic origin extended to an altitude of approximately 20 km. With only the above information it is therefore difficult to determine a reliable model of the aerosol layers for the time of the December 1963 eclipse.

In addition to the above uncertainty in the vertical distribution of aerosols, weather conditions at various local areas may affect the density near the central region of the umbra, as discussed in Section IV-E. Indeed, it has been reported that at the time of the December 1963 eclipse the

effective part of the terminator was partially cloudy [Brooks, 1964]. As shown by Tiros photographs on that date, although the cloud regions were highly variable, they appear to produce appreciable extinction in the tropospheric region. It is reasonable to assume that such additional extinction caused by water particles would be most effective near the tropopause where the above discussed sink of aerosols was observed. In any case, the troposphere reaches to approximately 9 or 10 km on the average and therefore above 10 km there is no significant extinction due to water particles.

In adding the extinction due to aerosols and water particles, therefore, we considered various models with homogeneous distributions of spherical particles up to a certain height. The particles above 10 km are assumed to consist of aerosols and those below 10 km are mixtures of aerosols and water particles. The relative contribution of weather conditions to aerosol extinction may then be examined by taking different densities of the particles in the regions above and below 10 km. An advantage in the homogeneous distributions is seen in the discussion following equation (34). That is, homogeneous layers with the same upper and lower limits have identical values for $L(h_o)$ defined by equation (34), or $L(h_o)$ is

independent of the number density or the size of an average particle. Hence, different models are described by the single parameter, β, the vertical extinction coefficient for the combined dust and water particles. An assumed model may then be compared directly to the atmospheric extinction coefficient determined by the usual photometric observation.

C. Clear Sky with Normal Aerosol Extinction

The visual extinction in the vertical direction due to the normal content of aerosol particles is found to be $\beta^A = 0.07$ mag./air mass [Allen, 1963]. This value yields the total visual extinction of about 0.21 mag./air mass which corresponds to the clear sky condition at the average ground level observation. Figure 5 shows the shadow density computed for a model of aerosols extending to 25 km with $\beta = 0.07$ including both molecular and aerosol diffusion.

As compared to Figure 4, the red and green curves are lowered by at least 2.5 magnitudes near the central region and these decreases are much greater throughout the umbra than those due to changing the ozone content. It appears therefore that accurate measurements of the shadow density provide a clear means to determine aerosol contents in the upper atmosphere

at the time of an eclipse. We see in Figure 5 that the reddening effect is still present distinctively through the umbra, indicating that the assumed aerosol extinction is too small to explain the observed colors of the December 1963 eclipse.

D. Effect of Cloudy Sky

For the purpose of comparing the relative effects of a dust layer extending up to 25 km to those of a cloud layer which has a maximum altitude of 10 km the shadow density has been computed in each of these cases with the same β. Hence, the combined number density of both dust and water particles in the model extending to 10 km is two and one-half times as great as the other case, if the average particle size is the same in the two models. The results for green light for the cases, β = .10 and .22 mag./air mass, are compared in Figure 6 which also includes the contribution from diffusion by molecules and both types of particles. The difference between the two models is seen to be extremely large, being about 5.7 magnitudes for β = .22 and 2.5 magnitudes for β = .10 at 30 minutes from the shadow center or 15 minutes from the umbra limb.

E. Aerosol Extinction Determined from December 1963 Eclipse Observation

Finally, it has been attempted to find a model which would agree exactly with the measurements of Matsushima and Zink for the 1963 eclipse, which consisted of V = 16.25 mag. with B-V zero or slightly negative near 10 minutes from the umbra center. As discussed before, after assuming homogeneous layers with the upper limit of 25 km, the shadow densities for various different models are obtained by changing the value of β. An average ozone content of 0.26 cm S.T.P. is taken for all models. The values of the shadow densities at the point 10 minutes from the umbral center thus obtained are listed in Table II. The effect of increasing β is very large in the visible region, but is rather small in the blue region. The small change in the blue color is due to the fact that the blue light in this region of the shadow is mainly due to the diffusion of light rather than to direct illumination by refracted light. From the comparison with the observation by Matsushima and Zink, we finally adopt the value of β between 0.20 and 0.22 to be the model which yields the best agreement with observation. The computed shadow densities in three colors are plotted in Figure 7.

VII. DISCUSSION AND CONCLUSION

From the determination of visual extinction coefficients over 18 months following the eruption of Mt. Agung, Moreno et al. [1965] found that the increase in extinction at Cerro Tololo, Chile, reached a maximum value of about 0.26 mag./air mass in late September 1963. By the end of December, the increase in extinction dropped to about 0.10 mag./air mass and it remained so thereafter. Our adopted value of $\beta = 0.21$ mag./air mass indicates an additional aerosol extinction of about 0.14 mag./air mass. Since a substantial fraction of this extinction is considered to be due to the dust layer below the altitude 2 km, and the Cerro Tololo Observatory is located at an elevation of 2.2 km, both results seem to be in good agreement. In fact, a similar increase and decrease of the extinction coefficient were observed by Praybylski [1964] at Mt. Bingar in Australia, but the absolute value of visible extinction is found to be about 0.03 mag./air mass larger than at Cerro Tololo during the period between September and December 1963. Noting that the elevation of Mt. Bingar is 0.46 km there seems to be a good agreement in this case, too.

It should be emphasized that the present results have been obtained without specifying the number density or the average size of the aerosol particles. The density of the particles is implicit in the final value of β, from which the product of the density and the square of the average particle radius may be determined (equation (31). We note that the assumption of the neutral extinction appears to be consistent with the observations of Mareno et al., as discussed before.

As compared to the various other sources of attenuation of light included in the present calculation, we note in Figure 4 that the effect due to a possible error in the adopted value of the ozone content appears to be small. Consequently, the determination of the ozone content from the eclipse observation requires very accurate photometry near the limb of the umbra. In Figure 6, we see that the effects of aerosol extinction and weather conditions would be easily distinguishable in the light density in the outer half of the umbra. The same figure also indicates that data in this region would serve as a means to determine the upper limit of the aerosol layer. Unfortunately, the only quantitative measurement of the December 1963 eclipse was by Matsushima and Zink and it was interrupted during the time the observed point was passing

through this region. The greatest approximation appears to lie in the use of the homogeneous distribution of spherical particles. As we mentioned before, however, the observed sink in the dust distribution below 10 km may be largely compensated by the presence of clouds near the same altitudes. Especially when we compare with the observed light density near the central region of the umbra only, the error due to the homogeneous models is reduced greatly because the light illuminating the central region comes from a wide range of altitudes as well as from practically the entire terminator circle.

In any case, the above results indicate that the primary cause for the unusually dark and non-reddened eclipse on December 30, 1963 was the additional extinction due to the volcanic dust ejected by the eruption of Mt. Agung. In such an unusually dark eclipse the diffusion of light becomes important in the central region of the shadow and in fact dominates the results in the blue and green wavelengths. It appears that in future eclipse observations accurate measurements near the limb of the umbra are extremely important in distinguishing the effects of different sources of light extinction. Above all, photometric measurements in the red color near the umbra limb appear to be most useful in determining the structure of the upper atmosphere.

VIII. ACKNOWLEDGEMENT

One of the authors (S.M.) wishes to thank Dr. F. Link of Czechoslovakia for his stimulating discussions and encouragement through correspondence. He is greatly indebted to Dr. H. Moreno in Chile, Dr. A. Przybylski in Australia, and Mr. J. M. Rosen at Minnesota who provided him with valuable data before publication.

REFERENCES

Albright, J., 1939, Phys. Meteorology (Prentice-Hall)

Allen, C. W., 1963, Astrophys. Quantities, 2nd Ed. (U. of London Press).

Altshuler, T., 1961, General Electric M.S.V.D., No. 61SD199.

Brooks, E., 1964, Sky and Telescope 27, 346.

Campen, C. (Editor), 1961, Handb. Geophys. (Macmillan).

Champion, K., W. O'Sullivan, and S. Teweles, 1962, U. S. Stand. Atmosph. (U. S. Government Printing Office).

Green, A. E. S., 1964, Applied Opt. 3, 203.

Humphreys, W., 1940, Physics of the Air, 3rd Ed. (McGraw-Hill).

Inn, E., and Y. Tanaka, 1953, J. Opt. Soc. Amer. 43, 870.

Link, F., 1963, Advances Astron. and Astrophys. ed. Z. Kopal, Vol. 2 (Acad. Press).

Matsushima, S., 1965, to be published.

Matsushima, S., and J. R. Zink, 1964, Astron. J. 69, 481.

Meinel, A., and M. Meinel, 1964, Nature 20, 657.

Moreno, H., N. Senduleak, and J. Stock, to be published.

Penndorf, R., 1957, J. Opt. Soc. Amer. 47, 176.

Przybylski, A., to be published.

Rosen, J. M., 1964, J. Geophys. Res. 69, 4673.

Rosen, J. M., 1965, Private Communication.

REFERENCES
(continued)

Svestka, Z., 1948, B.A.C. 1, 48.

van de Hulst, H., 1957, Light Scattering by Small Particles (John Wiley and Sons).

Vigroux, E., 1953, Ann. Phys. 8, 709.

TABLE I

Refraction, Refraction Gradient, and Tangential Air Mass and Ozone Quantity as a Function of the Minimum Altitude of the Light Ray.

h_o	ω	$R_o \frac{d\omega}{dh_o'}$	M	$O(h_o)$ (.26 cm S.T.P.)	$O(h_o)$ (.36 cm S.T.P.)
1	63.4	45230	73.7	6.23	8.62
2	57.8	41230	65.5	6.40	8.85
3	52.6	37600	58.2	6.57	9.10
4	47.7	34260	51.5	6.76	9.36
5	43.2	31220	45.5	6.96	9.64
6	39.1	28380	40.1	7.18	9.94
7	35.3	25730	35.2	7.41	10.25
8	31.8	23190	30.8	7.64	10.58
9	28.7	20520	26.9	7.89	10.93
10	26.2	14700	23.3	8.15	11.28
11	23.8	18600	20.2	8.41	11.64
12	20.8	23210	17.2	8.66	11.99
13	17.7	19390	14.6	8.91	12.34
14	15.0	16290	12.4	9.14	12.66
15	12.8	13660	10.6	9.34	12.94
16	10.9	11540	9.03	9.50	13.16
17	9.31	9738	7.69	9.60	13.29
18	7.94	8215	6.56	9.62	13.33
19	6.79	6848	5.60	9.56	13.24
20	5.81	5944	4.77	9.40	13.01
21	4.95	5266	4.07	9.12	12.63
22	4.20	4429	3.47	8.74	12.10

TABLE I
(continued)

h_o	ω	$R_o \frac{d\omega}{dh'_o}$	M	$O(h_o)$ (.26 cm S.T.P.)	$O(h_o)$ (.36 cm S.T.P.)
23	3.57	3734	2.96	8.26	11.43
24	3.04	3151	2.53	7.68	10.64
25	2.59	2661	2.16	7.04	9.75
26	2.20	2254	1.85	6.36	8.81
27	1.88	1906	1.58	5.67	7.85
28	1.61	1618	1.36	4.98	6.90
29	1.37	1371	1.16	4.32	5.98
30	1.17	1160	.998	3.71	5.13
35	.536	548	.466	1.52	2.11
40	.245	237	.226	.56	.77
45	.117	108	.114	.19	.27
50	.059	47	.061	.07	.09
55	.032	23	.033	.02	.03
60	.018	14	.018	.01	.01
65	.010	7	.009	.00	.00
70	.005	4	.005	.00	.00
75	.003	2	.002	.00	.00
100	.000	0	.000	.00	.00

TABLE II

Comparison of Shadow Density and Color at a Point 10 Minutes from the Shadow Center for Different Models of Aerosol Distribution.

β(mag./air mass)	D_{4600} (B)	D_{5400} (V)	B-V
0.00	15.197	11.353	3.844
0.07	16.098	13.945	2.153
0.10	16.199	14.896	1.303
0.20	16.255	16.244	.011
0.225	16.256	16.292	- .036

FIGURE CAPTIONS

Figure 1. Geometric relations between various integration variables.

Figure 2. Integration variables on the sun's disk as projected from the earth's atmosphere.

Figure 3. Shadow densities in three colors for a pure Rayleigh atmosphere. The contribution of molecular diffusion is appreciable only in blue color as indicated by the broken line.

Figure 4. Shadow density for the atmosphere including Rayleigh scattering and ozone absorption.

Figure 5. Shadow density for the atmosphere including a normal content of aerosol particles.

Figure 6. Comparison of shadow densities between atmospheric models with different vertical contents of aerosol particles.

Figure 7. Shadow density in the central region of the umbra for the atmospheric model adopted for the December 1963 eclipse.

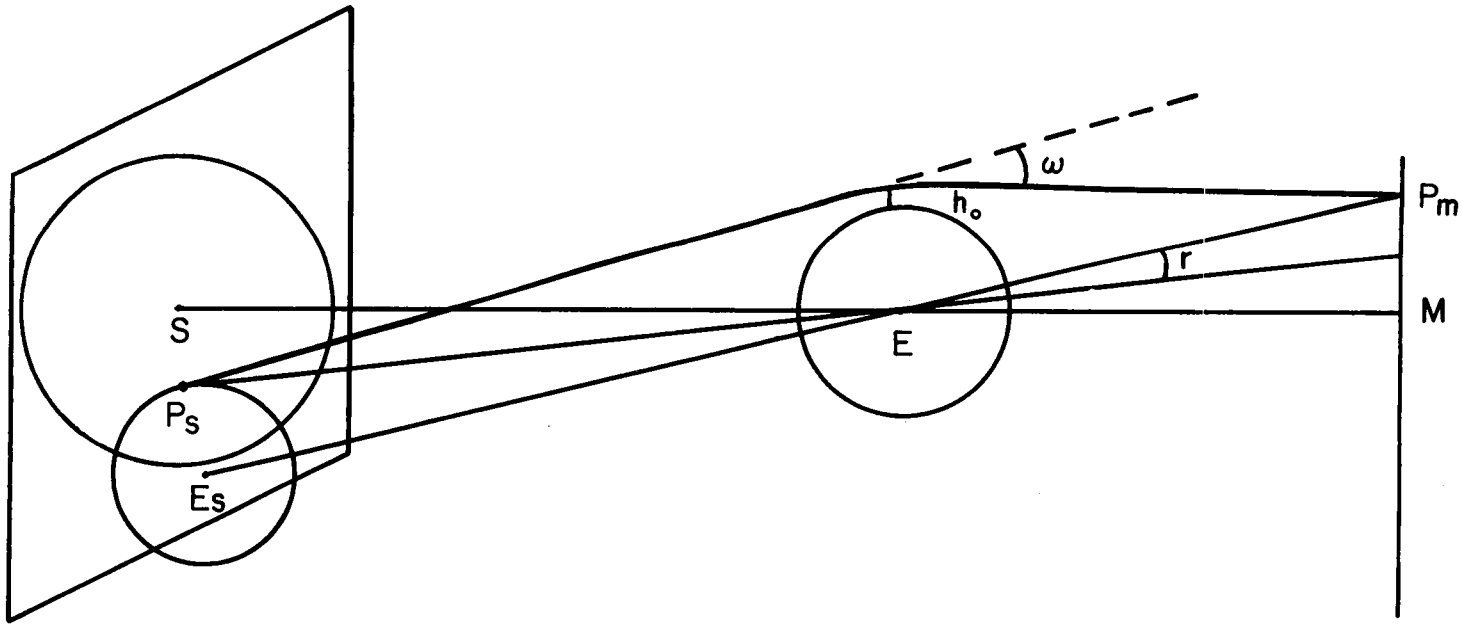

FIGURE 1

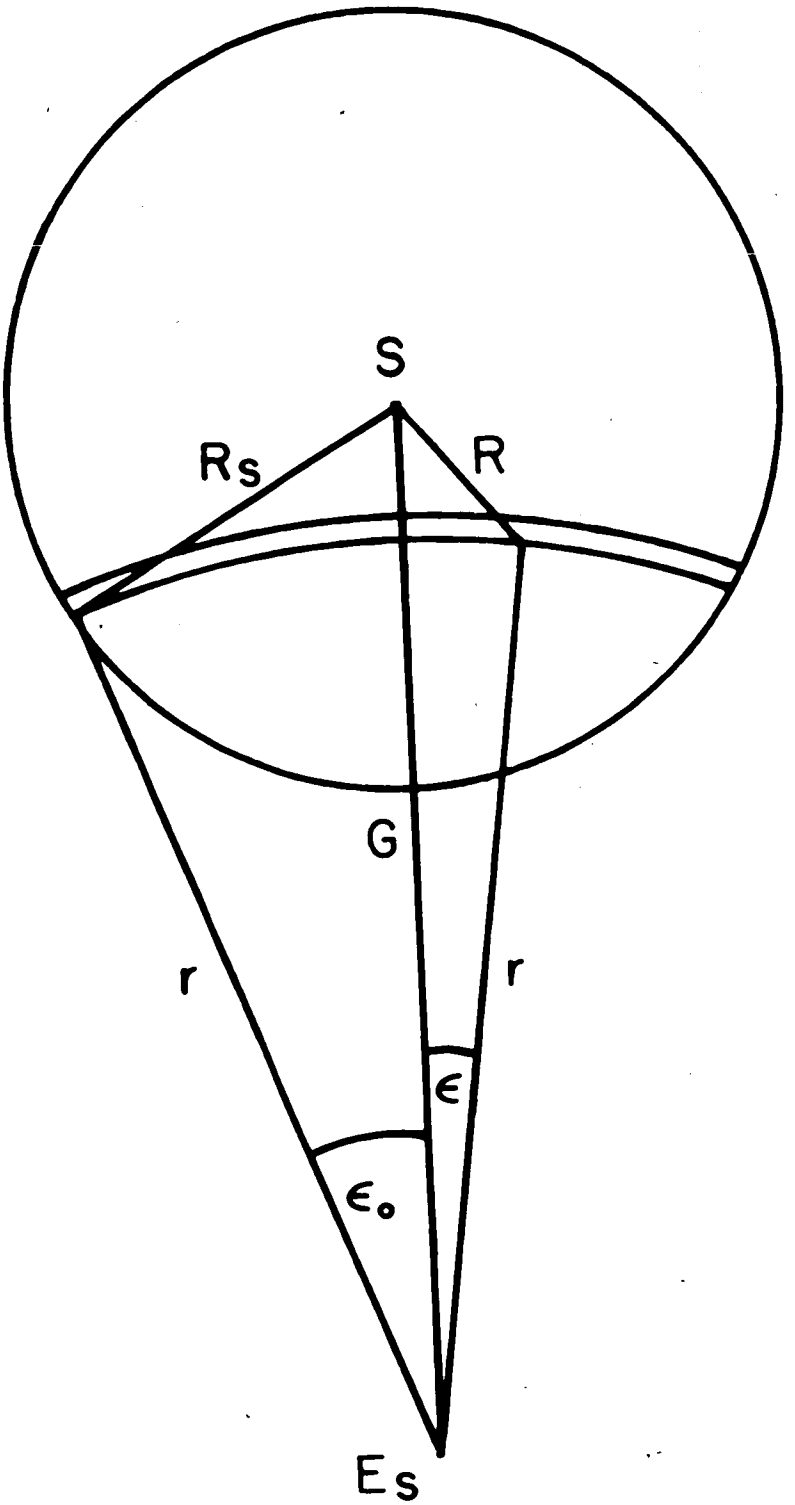

FIGURE 2

65-2,3

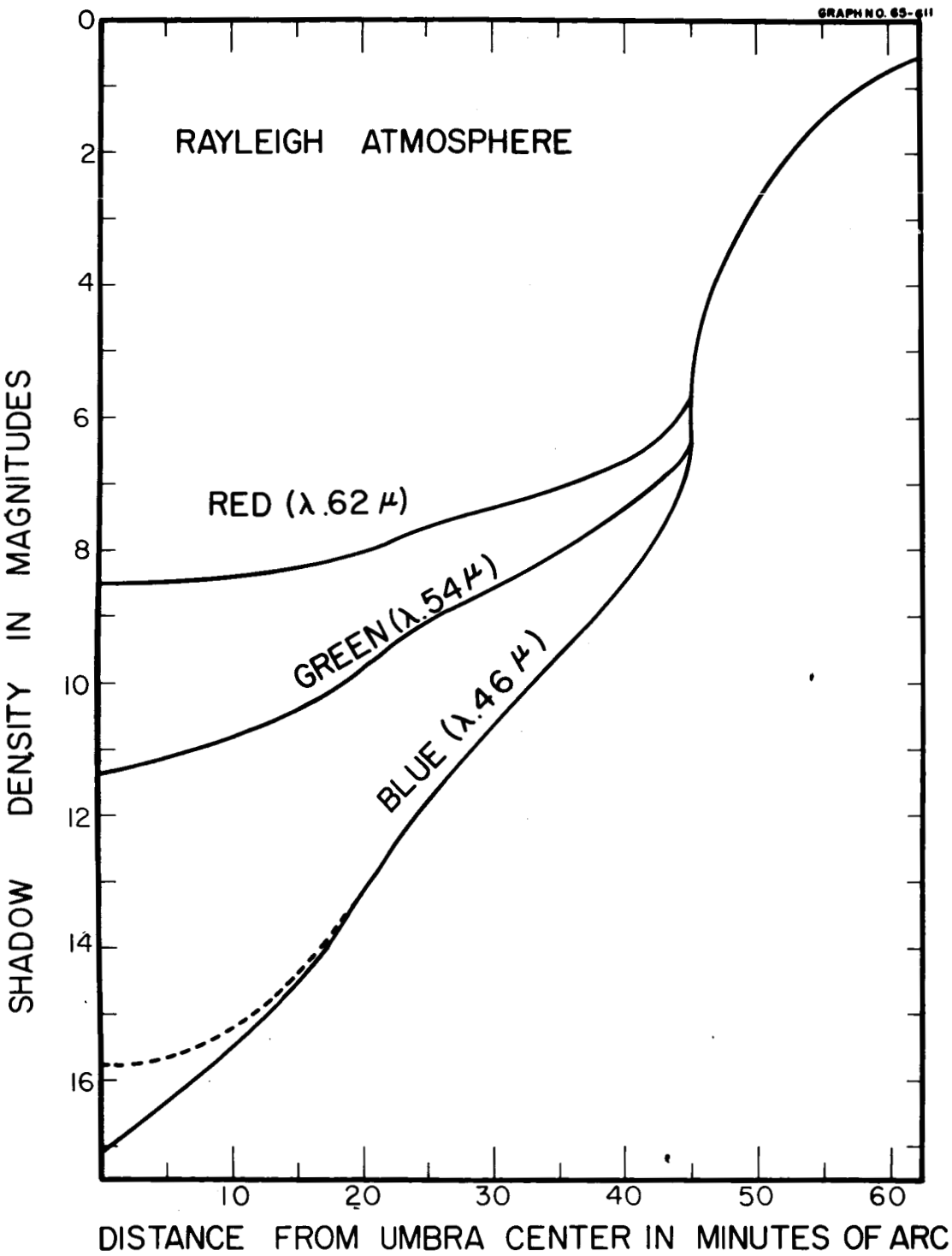

FIGURE 3

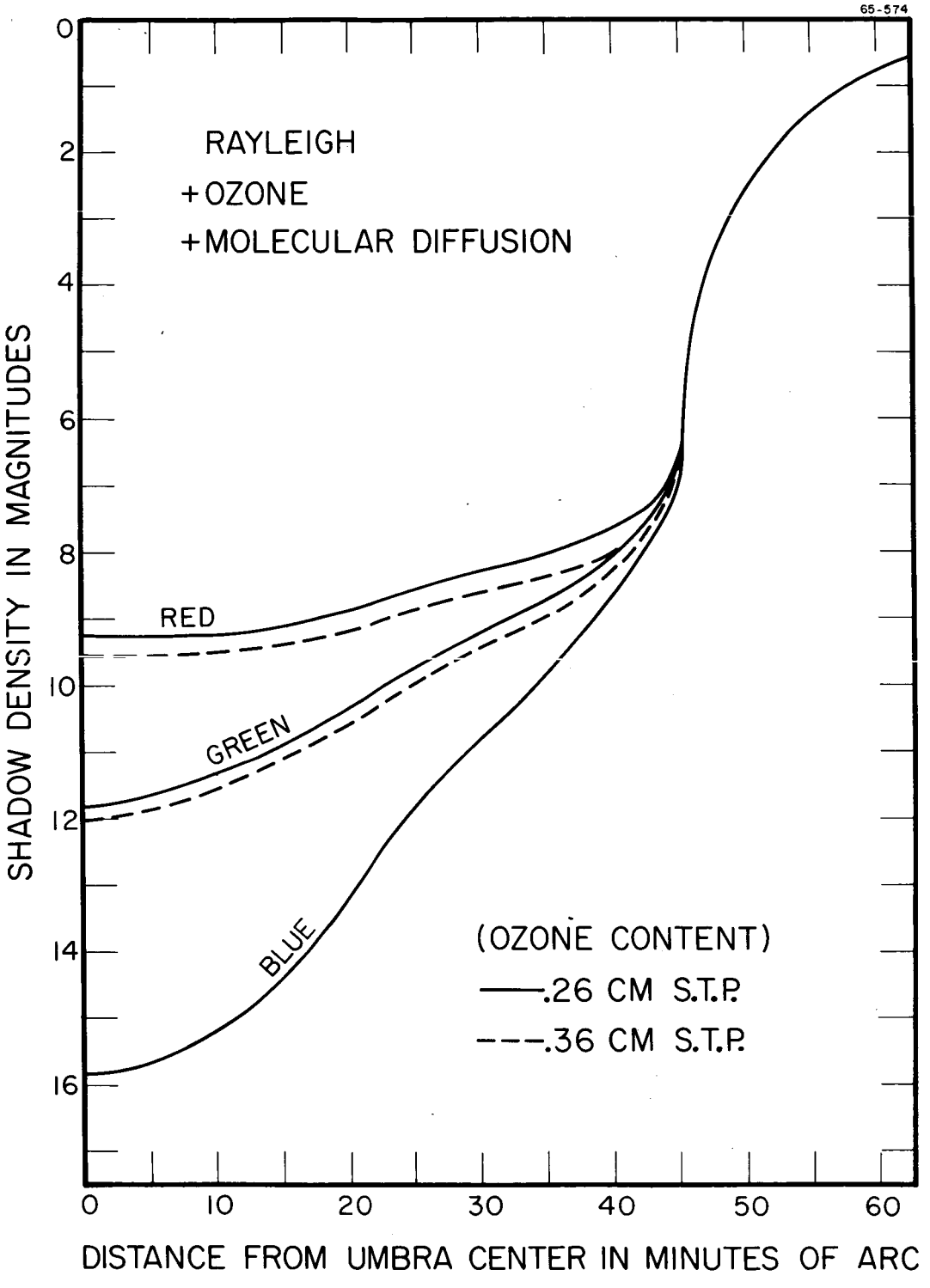

FIGURE 4

65-212

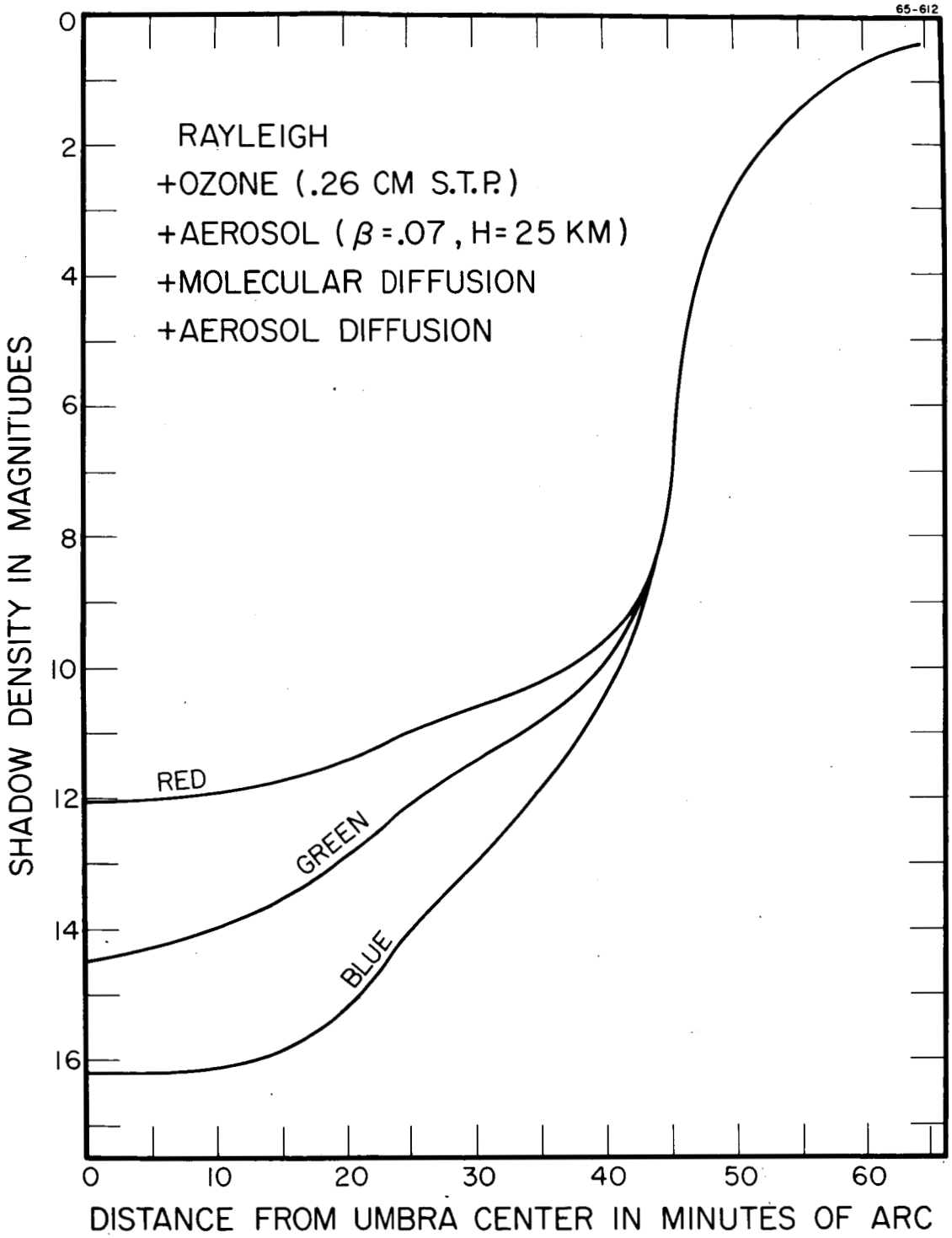

FIGURE 5

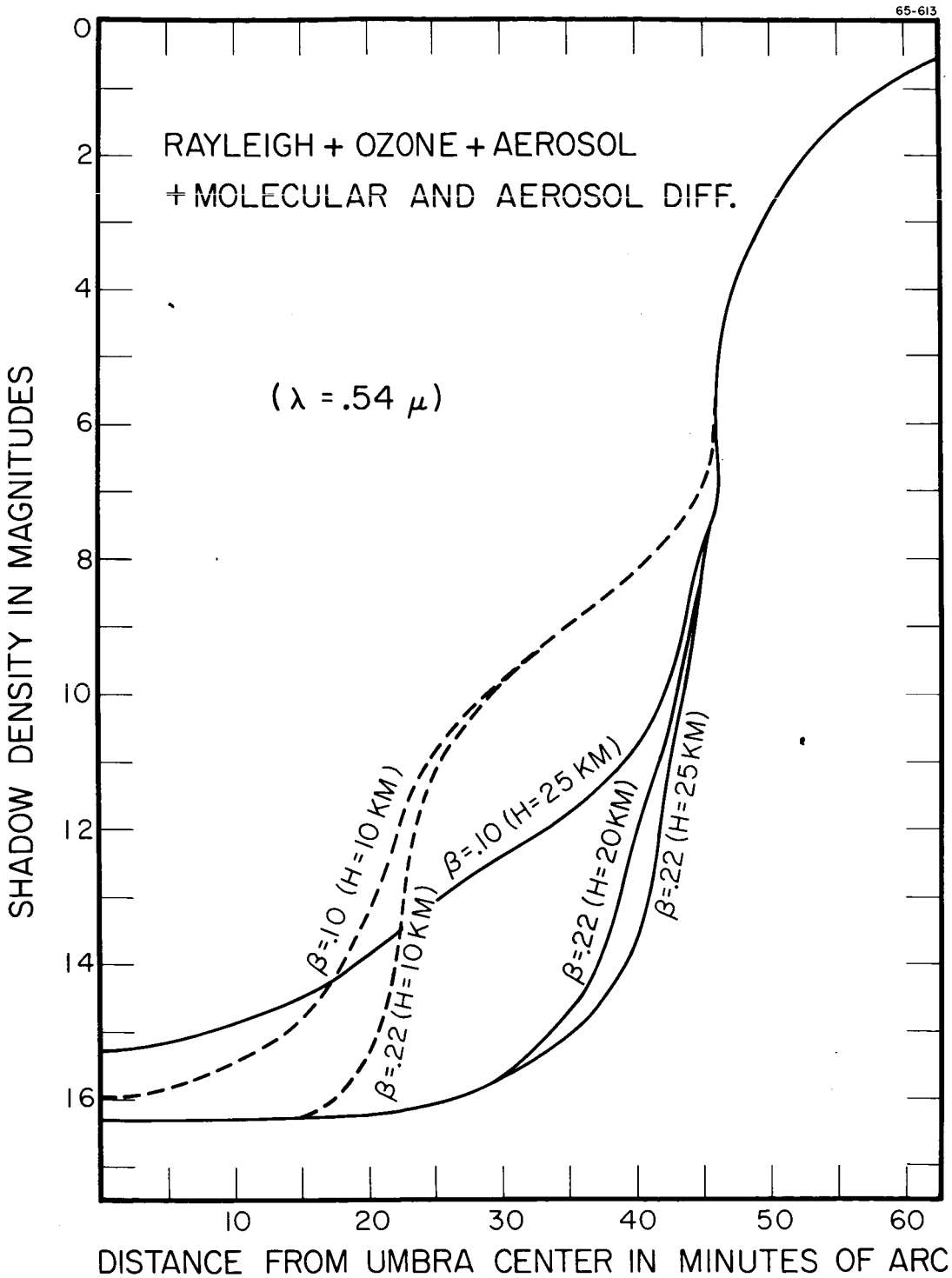

FIGURE 6

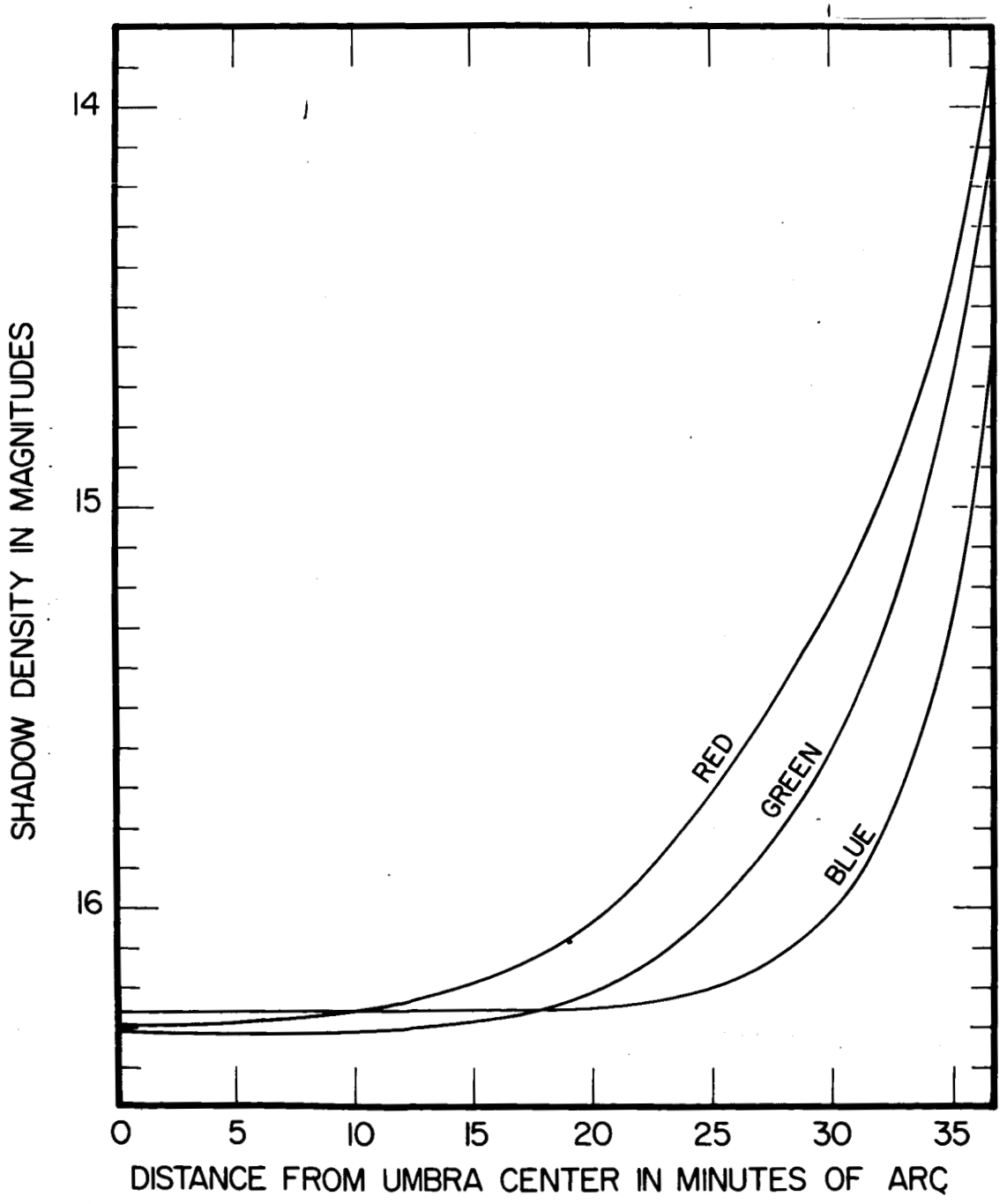
SHADOW DENSITY IN MAGNITUDES
14
15
16
RED
GREEN
BLUE
0
5
10
15
20
25
30
35
DISTANCE FROM UMBRA CENTER IN MINUTES OF ARC

FIGURE 7